



HAL
open science

On the dynamics in the southeastern Ligurian Sea in summer 2010

Pierre-Marie Poulain, Elena Mauri, R. Gerin, Jacopo Chiggiato, Katrin Schroeder,
Annalisa Griffa, Mireno Borghini, E. Zambianchi, P. Falco, Pierre Testor, et al.

► **To cite this version:**

Pierre-Marie Poulain, Elena Mauri, R. Gerin, Jacopo Chiggiato, Katrin Schroeder, et al.. On the dynamics in the southeastern Ligurian Sea in summer 2010. *Continental Shelf Research*, 2020, 196, pp.104083. <10.1016/j.csr.2020.104083>. <hal-02904210>

HAL Id: hal-02904210

<https://hal.science/hal-02904210v1>

Submitted on 9 Dec 2020

HAL is a multi-disciplinary open access archive for the deposit and dissemination of scientific research documents, whether they are published or not. The documents may come from teaching and research institutions in France or abroad, or from public or private research centers.

L'archive ouverte pluridisciplinaire **HAL**, est destinée au dépôt et à la diffusion de documents scientifiques de niveau recherche, publiés ou non, émanant des établissements d'enseignement et de recherche français ou étrangers, des laboratoires publics ou privés.



HAL Authorization

Continental Shelf Research

On the dynamics in the southeastern Ligurian Sea in summer 2010

--Manuscript Draft--

Manuscript Number:	
Article Type:	Research paper
Section/Category:	Physical Oceanography (estuarine, coastal and shelf sea - modelling and process studies)
Keywords:	Drifter, glider, Ligurian Sea, Corsica Channel, offshore-flowing filaments, wind-driven circulation
Corresponding Author:	Pierre-Marie Poulain OGS Sgonico, Trieste Italy
First Author:	Pierre-Marie Poulain
Order of Authors:	Pierre-Marie Poulain Elena Mauri Riccardo Gerin Jacopo Chiggiato Katrin Schroeder Annalisa Griffa Mireno Borghini Enrico Zambianchi Pier Paolo Falco Pierre Testor Laurent Mortier
Abstract:	<p>Drifters and a glider were operated in the southeastern Ligurian Sea to study the near-surface currents and water mass properties in summer 2010. Additional data were collected by a moored current meter in the Corsica Channel (CC). These in situ data were complemented by surface wind products, satellite images of chlorophyll concentration and a Regional Ocean Modeling System (ROMS) numerical model that was implemented to simulate the local coastal dynamics. Southward currents were prevailing along the continental Italian coast, advecting filaments with a high optical signal coming from the Arno River. North of Elba Island, currents turned westward and northward in the vicinity of the CC. Further to the north they veered eastward, forming an anticyclonic circulation feature centered around Capraia Island. This general circulation picture was disrupted and reversed during events of sustained southerly winds occurring with a period of about a week. The near-surface currents in the CC and the anticyclonic circulation around Capraia Island showed the same weekly variations related to the local wind forcing. The ROMS model simulations agreed satisfactorily with the observations, in particular the strength of the Capraia anticyclonic circulation (quantified with the Capraia index) was confirmed to be strongly wind-dependent.</p>
Suggested Reviewers:	Hezi Gildor hezi.gildor@mail.huji.ac.il Dan Hayes hayesdan@cyprus-subsea.com Nadia Pinardi nadia.pinardi@unibo.it Carlo Brandini brandini@lamma.rete.toscana.it



Sgonico, 13 September 2019

Dear Sir/Madam:

Please find attached a manuscript entitled "On the dynamics in the southeastern Ligurian Sea in summer 2010" that we would like to be considered for publication in the Continental Shelf Research.

Sincerely yours.

Dr. Pierre-Marie Poulain

Head, Mobile Autonomous Oceanographic Systems (MAOS)

Oceanography Section, OGS

Senior Scientist

Environmental Knowledge and Operational Effectiveness (EKOE), CMRE

1
2
3
4
5
6
7
8
9
10
11
12
13
14
15
16
17
18
19
20
21
22
23
24
25
26
27
28

On the dynamics in the southeastern Ligurian Sea in summer 2010

^{1,2}Poulain P.-M., ¹Mauri E., ¹Gerin R., ³Chiggiato J., ³Schroeder K., ⁴Griffa A., ⁴Borghini M.,
^{5,6}Zambianchi E., ⁵Falco P., ⁷Testor P., ⁷Mortier L.

¹Istituto Nazionale di Oceanografia e di Geofisica Sperimentale (OGS), Trieste, Italy

²Center for Maritime Research and Experimentation (CMRE), La Spezia, Italy

³Istituto di Scienze Marine (ISMAR), CNR, Venezia, Italy

⁴Istituto di Scienze Marine (ISMAR), CNR, La Spezia, Italy

⁵Università Parthenope, Naples, Italy

⁶Istituto di Scienze Marine (ISMAR), CNR, Rome, Italy

⁷Laboratoire d'Océanographie et du Climat (LOCEAN), Paris, France

Corresponding author:

P.-M. Poulain,
OGS, Borgo Grotta Gigante, 40/c,
Sgonico (TS), Italy
(ppoulain@inogs.it)

Continental Shelf Research

September 2019

Keywords: Drifter, glider, Ligurian Sea, Corsica Channel, offshore-flowing filaments,
wind-driven circulation

Highlights

29

30

31

- The surface circulation in the southeastern Ligurian Sea is strongly wind-dependent.

32

33

- Anticyclonic circulation around Capraia Island is predominant.

34

- Currents transport offshore filaments of low-salinity and nutrient-rich waters of riverine origin.

35

36
37
38
39
40
41
42
43
44
45
46
47
48
49
50
51
52
53

Abstract

Drifters and a glider were operated in the southeastern Ligurian Sea to study the near-surface currents and water mass properties in summer 2010. Additional data were collected by a moored current meter in the Corsica Channel (CC). These in situ data were complemented by surface wind products, satellite images of chlorophyll concentration and a Regional Ocean Modeling System (ROMS) numerical model that was implemented to simulate the local coastal dynamics. Southward currents were prevailing along the continental Italian coast, advecting filaments with a high optical signal coming from the Arno River. North of Elba Island, currents turned westward and northward in the vicinity of the CC. Further to the north they veered eastward, forming an anticyclonic circulation feature centered around Capraia Island. This general circulation picture was disrupted and reversed during events of sustained southerly winds occurring with a period of about a week. The near-surface currents in the CC and the anticyclonic circulation around Capraia Island showed the same weekly variations related to the local wind forcing. The ROMS model simulations agreed satisfactorily with the observations, in particular the strength of the Capraia anticyclonic circulation (quantified with the Capraia index) was confirmed to be strongly wind-dependent.

54 **1. Introduction**

55 Currents and transports of water mass properties in sea areas including islands and channels
56 and in the coastal zone are crucial at the local scale for the dispersion and mixing of pollutants
57 and at the large scale for the interaction between different basins, which in turn can control
58 the whole functioning of entire seas or oceans. Besides, if important river mouths co-exist in
59 the vicinity of islands and channels, the distribution of the water masses and the local
60 ecosystem dynamics can even be more complex and challenging to monitor and study.

61

62 The Mediterranean area in the southeastern Ligurian Sea and northern Tyrrhenian Sea (Fig.
63 1), connected by the Corsica Channel (CC), is such an area, with complex topography and
64 coast morphology, the existence of several islands (Elba, Monte Cristo, Giglio, etc) and also
65 the mouth of an important Italian river (the Arno River). Fluxes across the CC have been
66 measured almost continuously between 1982 and 1998 with moored currentmeters (Manzella,
67 1984; Astraldi et al., 1990; Astraldi and Gasparini, 1992). The northward flowing current in
68 the CC, also referred to as the Tyrrhenian (Astraldi and Gasparini, 1992) or Eastern Corsica
69 Current (ECC, Pinardi et al. 2006), is maximum in winter and is mainly driven by the steric
70 sea level difference between the Tyrrhenian to the south and the Ligurian Sea to the north.
71 This difference is larger in winter due to the larger heat loss and the local effect of the wind
72 stress curl in the Liguro-Provençal basin (Pinardi and Masetti, 2000). The heat flux
73 associated with the ECC varies seasonally and plays a crucial role for deep water formation
74 processes in the NW Mediterranean (Astraldi and Gasparini, 1992). The ECC is characterized
75 by velocity fluctuations with periods between 2 and 15 days with the occurrence of
76 intermittent reversals (Astraldi et al., 1990).

77

78 This ECC seasonal (and also inter-annual) variability was confirmed by satellite altimetry
79 data along selected satellite sub-tracks criss-crossing in the CC vicinity (Vignudelli et al.,

80 1999, 2000, 2005; Bouffard et al., 2008). Vignudelli et al. (1999) have shown that the
81 interannual variations of water transport through the CC, as measured by satellite altimeters,
82 can be related to the North Atlantic Oscillation. More recently, Bouffard et al. (2008) have
83 demonstrated that multi-mission altimetric data agree well with in-situ measurements and
84 therefore represent an accurate long-term mean to monitor the exchange between the
85 Tyrrhenian and Ligurian seas.

86

87 Conductivity-temperature-depth (CTD) measurements and numerical simulations (Onken et
88 al., 2005) as well as surface drifters (Poulain et al., 2012) have shown that the ECC can veer
89 in the clockwise sense around Capraia Island and form an anticyclonic eddy centered around
90 the island. We will refer to this circulation feature as the Capraia anticyclone, although it has
91 recently been also named “Ligurian Anticyclone” by Ciuffardi et al. (2016). It appears to be
92 dominant in summer when the ECC is weak. In particular, one drifter in summer 2007
93 completed 5 full loops around the island with a periodicity of about 3 days (Poulain et al.,
94 2012).

95

96 In this paper, simultaneous observations of currents and water mass properties obtained by a
97 glider, surface drifters and moored instruments, along with ancillary satellite data and wind
98 products and numerical model simulations, are used to explore and study the dynamics of the
99 southeastern Ligurian and CC in summer 2010. Most data were collected as part of the
100 LIDEX10 campaign, whose general objective was to improve the understanding of turbulent
101 transport and dispersion in the ocean, more specifically to study the dispersion in a coastal
102 frontal zone due to mixing by meso- and submesoscale structures (Schroeder et al., 2012).
103 The main focus of this paper is on mesoscale (~10 km) and submesoscale (< 10 km)
104 structures, some of them transporting offshore and mixing the fresh and nutrient-rich waters
105 of river origin. The Capraia anticyclone, which has a subbasin scale (40-50 km), is described

106 quantitatively using the drifter data. Some aspects of the near-surface circulation and ECC
107 transport are also investigated, relating them to the local wind forcing.

108

109 Details about the instruments used and the collected data are provided in section 2. The
110 surface circulation as measured by the drifters is described in section 3.1, including a
111 qualitative description of their motions and a quantitative study of the Capraia anticyclone.
112 The effect of the local wind forcing is explored in section 3.2, using both observations and
113 numerical simulations obtained with the Regional Ocean Modelling System (ROMS). The
114 surface circulation derived from ocean color satellite images superimposed with drifter tracks
115 is discussed in section 3.3. Section 3.4 includes the results on the 3D spatial structure and
116 temporal evolution of the water mass properties (temperature and salinity) provided by the
117 glider and also detected in ocean color satellite images. Discussion of the most salient results
118 and conclusions are found in section 4.

119

120 **2. Data and methods**

121 The LIDEX10 experiment took place on-board the R/V Maria Grazia of the Italian National
122 Research Council (CNR) on 3 July 2010 in the southeastern Ligurian Sea off the Tuscany
123 coast (Italy). First, a conductivity-temperature-depth (CTD) survey was carried on, along a
124 zonal transect at latitude $43^{\circ} 35.34'$ N and between longitudes $9^{\circ} 56.7'$ E and $10^{\circ} 5.94'$ E,
125 including 12 casts down to 50 m depth and separated by 1-4 km. The CTD data revealed a
126 near-surface vertical front in the top 7-8 m below the surface, separating lower salinity and
127 higher chlorophyll fluorescence water inshore from saltier and poorer water offshore
128 (Schroeder et al., 2012). The CTD data are not discussed any further in this paper since the
129 glider repeated the same transect shortly after.

130

131 *2.1 In-situ observations*

132 2.1.1 Drifters

133

134 Two groups of 9 drifters were deployed after the CTD transect on 3 July 2010, on each side of
135 the front, approximately 5 km apart. For each group, the drifters were released in three tight
136 triplets separated by 300-500 m, and with 50-100 m distance between the drifters within each
137 triplet (see Fig. 2 of Schroeder et al., 2012). An additional drifter was deployed between the 2
138 groups on the front. In brief, the 19 drifters were deployed with relative distances ranging
139 from 50 m to 6 km. The deployments were conducted in less than 4 h (from 11:34 to 15:26
140 GMT). All drifters were CODE designs (Poulain, 1999; Poulain and Gerin, 2019), fitted with
141 GPS receivers and manufactured by Technocean (Cape Coral, Florida). They measure the
142 currents in the top first meter below the surface with an accuracy of 1-2 cm/s. The principal
143 error is a wind-induced slip of about 0.1% of the wind speed (Poulain and Gerin, 2019). Most
144 of the drifters (17 units) transmitted their data to the Argos system on-board polar-orbiting
145 satellites, whereas 2 drifters used the Iridium telemetry system. GPS positions and ancillary
146 data (e.g., sea surface temperature, battery voltage) were transmitted every hour.

147

148 The drifter GPS data were quality controlled and interpolated at 0.5 h intervals using a kriging
149 technique (see Menna et al., 2017 and references therein). Velocities were calculated by finite
150 differencing the interpolated positions (central difference scheme with hourly interval). For
151 some applications (see section 3.2) the drifter velocity timeseries were low-pass filtered with a
152 Hamming filter (36 h) to remove high frequency motions.

153

154 The mean half-life of the 19 drifters deployed on 3 July 2010 is about 2 weeks (many drifters
155 stopped on 19-21 July after 16-18 days). Unfortunately, the single drifter deployed between
156 the two clusters was rather short lived and stopped functioning on 7 July.

157

158 2.1.2 Glider

159 A shallow water Slocum glider manufactured by Teledyne Webb Research, Falmouth,
160 Massachusetts was deployed at location $43^{\circ} 35.78' N$, $10^{\circ} 06.20' E$ on 3 July 2010, shortly
161 after the drifter deployments (i.e., at 16:29 GMT). The glider was equipped with an un-
162 pumped Sea-Bird Scientific SBE 41 CT to measure conductivity (0.0003 S/m), temperature
163 ($0.002^{\circ} C$) and pressure (0.5 psi), along with sensors to measure dissolved oxygen, particle
164 backscattering and coloured dissolved organic matter fluorescence. It was programmed to
165 measure vertical properties of the water column as deep as 200 m. All sensors were set to
166 record every 8 seconds. The typical horizontal resolution of the glider data along its route was
167 about 0.5 km. In this paper only temperature, salinity and density observations are considered
168 to describe the local dynamics, with a main focus on the top 40 m of water.

169

170 The glider was initially piloted to sample the transect surveyed by the research vessel. Given
171 the southward motion of the drifters, and in order to have the glider and drifters in the same
172 area at about the same time, the glider was subsequently programmed to survey the
173 southeastern Ligurian Sea in a southward zig-zag pattern until it approached the northern
174 coast of Elba Island (Fig. 1). At this point it was piloted to move westward and to sample the
175 CC, until it was recovered on 20 July 2010 (at about 10:00 GMT) at $43^{\circ} 00.90' N$, $09^{\circ} 35.82'$
176 E, between the northern tip of Corsica and Capraia Island.

177

178 2.1.3 Mooring

179 A mooring with current meters is maintained by CNR ISMAR in the CC (between the
180 northern tip of Corsica and Capraia Island) since 1985. Its location is $43^{\circ} 1.5' N$, $9^{\circ} 41.0' E$.
181 Current profiles are measured with an upward 75 KHz RDI Acoustic Doppler Current Profiler
182 (ADCP), with a bin size of 16 m, between 32 and 384 m at 2 h intervals. The meridional and

183 zonal velocities were extracted from the dataset for the period July-August 2010. Only the
184 meridional (along-channel) component is considered here, since it is more significant for our
185 scopes than the zonal (across-channel) component (the meridional speed is on average 3 times
186 stronger than the zonal one), and gives indication on the water exchange between the
187 Tyrrhenian and the Ligurian Sea. For comparison with the surface drifter data, the mooring
188 data near 32 m depth was considered. In order to remove high frequency fluctuations, a
189 Hamming filter with cut off period of 36 h was applied to the velocity time series.

190

191 *2.2 Remotely sensed data*

192 Moderate Resolution Imaging Spectroradiometer (MODIS) satellite images of chlorophyll
193 concentration of the study area were used to describe the spatial structure and temporal
194 evolution of the surface circulation assuming that chlorophyll is a passive tracer advected by
195 the surface horizontal currents. Images of chlorophyll concentration were preferred on sea
196 surface temperature images as they delineate better the circulation features at meso- and
197 submesoscales (better contrast). Being in a coastal area where a river outflows nutrient-rich
198 water, there is a sharp contrast between coastal and offshore waters, the former being richer
199 (higher chlorophyll) and slightly colder (by about 1 °C, in our case). The daily images have a
200 horizontal resolution of 1 km.

201

202 *2.3 Wind products*

203 Consortium for Small-scale Modeling (COSMO, <http://www.cosmo-model.org>) wind
204 products run by the Italian Air Force National Meteorological Center were obtained for the
205 study area in July and August 2010. In particular, the COSMO-ME gridded 10-m vector
206 winds with 7 km grid spacing were used to force the ROMS model and to relate the wind
207 forcing to the currents measured by the drifters and at the CC mooring. For some applications
208 (see section 3.2) the COSMO-ME wind velocity timeseries were also low-pass filtered with a

209 Hamming filter (36 h) to remove high frequency fluctuations. Wind data at 10-m were also
210 obtained from the ODAS buoy (also called W1-M3A) located in the central Ligurian Sea (43°
211 48' N, 9° 9.6' E).

212

213 *2.4 Numerical simulations*

214 The ocean model employed in this application is the ROMS (Haidvogel et al., 2008;
215 Shchepetkin and McWilliams, 2005). As part of LIDEX10, the model was set up in
216 operational forecast mode on a domain covering the entire Ligurian Sea. The horizontal
217 resolution is 2 km, with 32 vertical sigma-levels non-linearly stretched to resolve the surface
218 boundary layer. The ocean model was forced by the COSMO-ME 10-m winds. Open
219 boundary conditions were applied to tracers and baroclinic velocity with radiation and
220 nudging (Marchesiello et al. 2001) from daily averages of the large-scale Mediterranean
221 Forecasting System (MFS) forecasts (Oddo et al., 2009). Three major rivers were included:
222 the Arno (daily discharges), Serchio and Magra (monthly climatologies). The operational
223 ROMS-based system was initialized on 1 May 2010 using an analysis field from the
224 Mediterranean Forecasting System (MFS) model. Since then, ROMS was run in forecast
225 mode once a day (00:00 UTC) with output data every 3 h and forecast range of 72 h. Data
226 assimilative analysis fields from the forecast system are available in Mourre and Chiggiato
227 (2014), but just for a short period. Thus, for this work only the free run (i.e., without data
228 assimilation) is considered. Additional details on the physics and numerical details
229 implemented in this application and performance can be found in Alvarez et al. (2012),
230 Schroeder et al. (2012), Mourre et al. (2011) and Mourre and Chiggiato (2014).

231

232 **3. Results**

233 *3.1 Surface circulation*

234

235 After deployment, all drifters moved southward, with the coastal group (red tracks in Fig. 2)
236 going faster and reaching 43°N latitude after 4 days, on 7 July. The other group (blue tracks in
237 Fig. 2) followed with about 1-day delay. Between 7 and 10 July the coastal group proceeded
238 westward towards the CC, and veered southward upon approaching Corsica. In contrast, the
239 other drifters slowed down and stagnated just north of Elba Island for about 2 days (11-12
240 July). Most of these drifters then moved northward (in the ECC and also near the Italian
241 continental coast) on 13-14 July, before turning back and moving south and west starting on
242 15 July. On 15-19 July, the drifters in the southern part of the CC showed slow and rather
243 chaotic currents, except for 2 drifters which moved swiftly northward between the northern tip
244 of Corsica and Capraia Island on 14 and 19 July. Four drifters (blue tracks) moved to the
245 southwest rapidly on 19 July and joined the area of the CC.

246

247 After the recovery of the glider on 20 July, some drifters continued to provide data on the
248 surface circulation in the study area for about another month (not shown). The most striking
249 characteristics of the currents during that period are: 1) on 22 July, fast northward currents in
250 the CC; 2) on 23-25 July, reversal of this current with drifter moving south in the CC; and 3) a
251 prevailing anticyclonic circulation around Capraia Island mostly during the period 20 July -
252 17 August. No drifter moved north of 43° 30' N and only 3 drifters moved eventually to the
253 Tyrrhenian Sea south of 42° 30' N after some time. The composite plot of all the drifter
254 trajectories between 3 July and 27 August 2010 is shown in Fig. 3, with speed color-coded
255 along the trajectories. Fastest unfiltered currents reaching 90 cm/s occur north of the CC in
256 the ECC (near 43° 15' N). Southward currents sampled during the first few days after
257 deployment range in 30-40 cm/s. Currents in the anticyclonic circulation around Capraia
258 Island are mostly in the 30-60 cm/s range. In the “stagnant” areas north of Elba Island and in
259 the CC, the speed is bounded by 20 cm/s. Note that high frequency motions, shown as loops
260 in the tracks, are ubiquitous in most of the drifter data. These motions have speeds of 10-20

261 cm/s. Spectral analysis revealed that they correspond to near-inertial oscillations, tidal
262 motions and currents driven by sea breeze. These high frequency motions are not considered
263 in the rest of the paper since the main focus is on dynamics at meso- and submesoscales.

264

265 Pseudo-Eulerian statistics were calculated from the drifter data for the period 3 July to 27
266 August 2010 using bins of 0.05° latitude \times 0.05° longitude. The number of hourly drifter
267 observations in the bins is maximum (in excess of 500) north of Elba Island and in the
268 southern part of the CC (not shown). Mean currents are shown in Fig. 4. for bins with more
269 than 5 hourly observations. The strong anticyclonic circulation around Capraia Island is
270 striking with mean speeds reaching 30 cm/s. This feature is about 60-70 km in diameter and is
271 bounded by $9^\circ 30'$ E and $10^\circ 20'$ E in longitude and $42^\circ 50'$ N and $43^\circ 30'$ N in latitude. Its
272 center is just to the northeast of Capraia Island. The period of rotation is 5-10 days. In total,
273 eight drifters executed 13 loops in this structure between 19 July and 19 August (one month).
274 Two drifters executed 4 loops each.

275

276 Fig. 5 shows the geographical distribution of the variability of the surface currents with
277 respect to the mean pattern shown in Fig. 4. The eddy kinetic energy (see definition in
278 Poulain, 2001) is low in the eastern part of the study area and in the southern CC. It increases
279 near the northern tip of Corsica and the northern extension of the CC (in the ECC) and the
280 northern limb of the anticyclonic circulation around Capraia Island.

281

282 *3.2 Wind forcing, near-surface currents and numerical simulations*

283 The COSMO-ME wind products at the grid point nearest the CNR mooring in the CC (43°
284 $7.5'$ N, $9^\circ 37.5'$ E, see Fig. 1) were considered to study the variability of the near-surface
285 currents related to the wind forcing. As shown in Fig. 6, in addition to daily variations
286 corresponding to sea breeze (see thin curve in middle panel), the wind is alternating between

287 northerly and southerly regimes with a periodicity of about a week. More specifically, major
288 northerly wind events occurred on 19, 24 and 30 July and on 6 and 21 August. On 14, 22 and
289 29 July and 15-16 and 27 August, winds were primarily southerly. Fig. 6 shows that the low-
290 pass filtered currents at 32 m depth measured by the mooring in the CC respond to the local
291 wind forcing, i.e., major events of southerly (northerly) winds correspond to increased
292 northward (southward) velocity. The correlation with zero-time lag between the meridional
293 winds and currents is about 0.69, but it increases to 0.71 for a lag of 5 h. This means that the
294 currents are barely delayed with respect to the wind.

295

296 If we plot the low-pass filtered drifter meridional velocities versus time along with the low-
297 pass filtered near-surface meridional flow in the Corsica Channel (Fig. 6, bottom panel), it is
298 striking that most drifter speeds co-vary with the mooring data. In particular, during the
299 events of strong northward flow (and southerly winds) of 13-14, 22-23 and 28-29 July, most
300 drifters are moving northward with speeds up to about 50 cm/s (after low-pass filtering). On
301 18-19, 23-24 and 29-30 July under northerly wind forcing the majority of drifters are moving
302 southward and the upper current in the CC is reversed (southward). Note that the variance of
303 the drifter meridional velocity is much higher than the mooring data mostly due to the spatial
304 variability sampled by the drifters.

305

306 Fig.7 shows the average surface circulation in the Ligurian Sea in July - August 2010
307 produced by ROMS. The two-month average clearly suppresses all short-term variability and
308 the emerging picture is controlled by the permanent features in the area. The overall
309 circulation of the western Ligurian Sea is cyclonic. Surface Atlantic Water (AW) enters the
310 Ligurian Sea from the south, mostly from the Algerian basin through the Western Corsica
311 Current (WCC). As expected in summer, the ECC in the CC is weak, in good agreement with
312 the drifter data (Fig. 4). The resulting current proceeds northward as a geostrophic frontal

313 system becoming the so-called Northern Current (NC) in the northern Ligurian Sea. In the
314 eastern Ligurian Sea, the Capraia anticyclone, identifiable in Fig. 7 by the relative maximum
315 in sea surface elevation, was a robust permanent feature of summer 2010.

316

317 In order to test the relationship with wind impulses, a Capraia Index was defined as the
318 difference in sea surface elevation between points A and B (see location in Fig. 7, top panel);
319 thus, a value close to zero corresponds to a wide shelf current whereas a large positive value is
320 suggestive of a strong anticyclone. The choice of an index that included point C (see Fig. 7)
321 was discarded, as the difference in sea surface elevation with respect to A may be due to a
322 structured boundary current (i.e., the WCC) disregarding the existence of the anticyclone.
323 From the time-series of the Capraia index (Fig. 7, middle panel) it can be seen that (a) the
324 anticyclone grows in intensity from early July to the end of August and (b) significant wind
325 events have the ability to partially or totally suppress the feature, with the noticeable example
326 of the (southwesterly) storm on 14-15 August (see wind speed in Fig. 7 bottom panel). As the
327 wind impulse weakens however, the index is suggestive of a re-emergence of the feature. The
328 southerly wind event around 13-14 July is in good agreement with the reversal of the coastal
329 current revealed by the drifters (Fig. 2).

330

331 *3.3 Surface circulation and satellite images*

332

333 During the period of glider operation (3-20 July) only 8 MODIS images were partially cloud
334 free and provided a useful description of chlorophyll concentration and the associated near-
335 surface circulation. On the day of the drifter and glider deployments (3 July), there was a
336 rather well-developed area of water with high chlorophyll concentration off the continental
337 Italian coast from the Arno River mouth to about 43°N 15' (Fig. 8a). This increased optical
338 signal is related to the higher nutrients discharged by the river. The significant Arno plume

339 was probably the result of an event on high discharge rate (reaching nearly 200 m³/s) around
340 21 June 2010 (data courtesy of Regione Toscana). The image confirms that the two groups of
341 9 drifters were deployed in and outside the coastal layer. The next two days (4 and 5 July, Fig.
342 8b,c), while all drifters were moving southward, the coastal layer developed two instabilities
343 forming offshore-flowing (and also southward flowing) filaments near 43° 25' N and 43° 10'
344 N. On 8 July (Fig. 8d), these instabilities were well separated in latitude and showed cyclonic
345 veering, that is offshore and southward circulation. The rich water of the southern instability
346 was advected towards Elba Island and then westward towards Corsica. There is a particularly
347 good agreement between the chlorophyll structures and the drifter tracks.

348

349 The offshore-flowing instabilities rooted on the Italian continental coast were still present
350 between 10 and 19 July (Fig. 9) with various shapes and offshore extensions. The northern
351 one extended as far as the Gorgona Island. Others developed near and south of Elba Island,
352 but were away from the areas sampled by the drifters and glider. To the west, off Corsica, an
353 instability plume was evident on 12, 17 and 19 July (Fig. 9b,c,d). On 12 July (Fig. 9b) drifters
354 were even trapped in it as it developed more offshore (as far as east as 9° 45' E).

355

356 During its entire mission, the glider protruded in and out of the chlorophyll-rich waters. For
357 instance, on 8 July (Fig. 8d) it encountered richer waters near the surface at both extremities
358 of this southwestward transect.

359

360 *3.4 Water mass properties and geostrophic currents in the water column*

361

362 The distribution of temperature, salinity and density along the glider track is discussed here
363 below, with main focus on the top 40 m of water where most of the variability occurs.
364 Selected transect (1, 8 and 15, see location in Fig. 1) are considered for the sake of brevity.

365

366 During its entire operation, the glider revealed a near-surface mixed layer extending down to
367 5-10 m (Figs. 10-12) on top of a thermocline spreading between approximately 10 and 40 m.
368 Along the northernmost transect 1 (Fig. 10) the isotherms and isopycnals are inclined
369 (deepening going offshore to the W) and the corresponding geostrophic currents are directed
370 southward. Further to the south, along transect 8 (Fig. 11), the above-mentioned iso-curves
371 are characterized by a concave upward structure. Qualitatively, the geostrophic currents are to
372 the SW in the eastern portion, where the drifters also move to the S and SW (see Fig. 8d).
373 More offshore (to the W) the currents are reversed, thus representing a mesoscale anticyclonic
374 circulation feature. In the southern part of the CC, along the zonal transect 15 (Fig. 12), the
375 isotherms and isopycnals correspond to concave downward. Again this is compatible with the
376 southward motion of the drifters near Corsica, and the usual northward direction of the ECC,
377 which is rather weak in summer.

378

379 Low-salinity water of Arno River origin (as demonstrated before in satellite images) extends
380 almost across the entire section but most importantly for distances larger than 2 km from the
381 westernmost point (Fig. 10). Water with salinity less than 37.6 prevails in the top 5-m layer.
382 Below it, the salinity is gradually increasing and reaching values in excess of 38.0 around 40
383 m depth. This is a signature of the upper core of the Levantine Intermediate Water which can
384 reach salinity of 38.6-38.7 at depths of 300-500 m in the Ligurian Sea (Bosse et al., 2015).
385 Besides the above-described features, the high horizontal resolution of the glider allowed to
386 sample a vein of relatively low salinity (~37.6) expanding offshore along transect 1 (Fig. 10)
387 between 10 and 25 m depth. The inclination of the vein is compatible with the slope of the
388 isopycnals and indicates the subduction of coastal water.

389

390 Along transect 8 the near surface salinity above 10 m has two minima (near 37.0) at the
391 extremities, corresponding to the Arno River plume extending offshore (to the east), and
392 presumably to the Atlantic Water coming from the CC (to the west). This low-salinity water
393 is also seen in transect 15 across the CC, although a little bit deeper (5-10 m) and capped
394 partially by saltier water.

395

396 In the CC (eastern part of transect 15), the glider data show consistent northward currents in
397 the entire depth range (0-200 m) whereas the mooring currents (Fig. 13) show mostly
398 northward currents above 80 m, with intensification on 13-14, 22 and 29 July and 14-15
399 August. Below, there are 1-2 weeks long periods of flow reversal, the most prominent one
400 lasting from 14 to 25 July and involving the water column up to 60 m depth. The surface
401 northward velocities average was 11.2 ± 7.4 cm/s, while the southward ones were much weaker
402 (-2.8 ± 2.6 cm/s).

403

404

405 **4. Discussion and conclusions**

406

407 During summer 2010, surface drifters and a glider were operated simultaneously to explore
408 the dynamics of the southeastern Ligurian Sea where the wind forcing, the local
409 geography/bathymetry and the outflow of the Arno River are supposed to affect significantly
410 the circulation and the distribution of the water mass properties. The glider was piloted in
411 order to obtain information in the water column in the area sampled by most of the drifters.
412 Ancillary data were obtained from a permanent mooring in the CC and from satellites
413 (MODIS images of chlorophyll concentration). In addition, a ROMS numerical model was
414 used to simulate the local dynamics and to help with the interpretation of the collected data.

415

416 The drifters revealed a surface circulation strongly affected by the local winds. Southward
417 currents dominated off the Italian continental coast. These currents reversed on 13-14 July due
418 to a change in wind direction, changing to southerly. The fluctuation of surface currents
419 between the southward and northward directions is seen in the drifter tracks over the entire
420 study area (in particular in the vicinity of Capraia Island) and in the near-surface records of
421 the mooring in the CC (see Fig. 6) during July and August 2010. The typical period of these
422 oscillations is one week.

423

424 Some drifters eventually depicted a strong anticyclonic circulation pattern centered on
425 Capraia Island (the Capraia anticyclone) starting on 20 July. The rotation period of these
426 drifters is 5-10 days, that is, slightly longer than the value (3 days) reported by Poulain et al.
427 (2012). Both drifters (Fig. 2) and the simulated sea surface height (Capraia index in Fig. 7)
428 showed an enhancement of the Capraia anticyclone in late July and August, only interrupted
429 by a storm on 14-15 August. This trend is related to the increase of negative vorticity of the
430 winds from July to August (not shown). On 14-15 August, strong winds from the SW
431 disrupted this trend and the anticyclone essentially vanished. In conclusion, ROMS numerical
432 model successfully simulated the occurrence of the Capraia anticyclone as a semi-permanent
433 and strengthening feature during July-August 2010, corroborating the hypothesis of the
434 significant role played by wind-storms in perturbing this eddy as well as the surface
435 circulation in the area.

436

437 The southward coastal currents advected the plume of the Arno River and associated
438 filaments of nutrient-rich waters towards the south, forming a layer of high chlorophyll
439 concentration along most of the Italian continental coast. This layer became unstable and
440 offshore-flowing filaments were generated typically at two locations between the Arno mouth
441 and Elba Island (see for instance Fig. 8d.). The northernmost filament reached almost the area

442 near Gorgona Island (Fig. 9d) and the southern one was advected near the northern coast of
443 Elba Island, into the CC and around Capraia Island (Fig. 8c,d).

444

445 The temperature, salinity and density data provided by the glider between 3 and 20 July 2010
446 show stratified conditions typical of summer with a surface mixed layer down to 10-20 m, a
447 thermocline expanding down to a maximum depth of 40 m. In terms of salinity, horizontal
448 variability (fronts) associated with the Arno plume and/or the AW occur along most transects.
449 For the Arno plume and its extension into offshore-flowing filaments, there is a good
450 agreement between the satellite chlorophyll images and the glider data. In the thermocline, an
451 inclined intrusion of fresher water (probably of Argo River origin) observed in transect 1 (Fig.
452 10) corresponds to subduction along isopycnals. Below 40 m, the increase of salinity with
453 depth represents the upper part of the LIW.

454

455 Currents measured at the CNR mooring in the CC corroborated the fluctuations of the near-
456 surface circulations with events of northward flow on 13-14, 22 and 29 July and 14-15 August
457 also experienced by the drifters (Fig. 13). Deeper in the water column, southward reversing
458 flow was observed for longer period (1-2 weeks) and rather independently from the surface
459 variability. These flow reversal events have already been reported by Astraldi et al. (1990).
460 They are not forced by the local winds but are probably related to the sea level difference
461 between the Tyrrhenian and Ligurian Sea.

462

463 The combined use of data provided by mobile and fixed autonomous instruments (drifters,
464 glider, mooring), by environmental satellites and numerical simulations in the southeastern
465 Ligurian Sea exemplifies an efficient way of collecting oceanographic data in this complex
466 sea area at relatively low costs. Obviously, a better sampling approach could have involved
467 data collection with more than one glider, the deployment of fixed moorings at key locations,

468 and an extensive survey of the entire study area with a research vessel. The study of coastal
469 dynamics as described in this paper, nevertheless, is a good example of multi-platform and
470 multi-parameter approach, which is the future paradigm in observational oceanography.

471

472 **Acknowledgements**

473

474 The authors are grateful to all the people who helped with the drifter and glider
475 deployment/recovery operations and with the data processing, and in particular to P. Zanasca,
476 A. Bussani, M. Menna, I. Mancero-Mosquera and K. Mahiouz. The drifters used in LIDEX10
477 were kindly provided by the NATO NURC Center (La Spezia, Italy), CNR, University
478 Parthenope of Naples and OGS. The glider (TENUSE) was contributed by LOCEAN. The
479 satellite data were downloaded from <https://modis.gsfc.nasa.gov/data/dataproduct/>. ODAS wind
480 data were provided by the EU FP7 EuroSITES project. COSMO-ME data were kindly made
481 available by CNMCA in Rome, Italy. Arno River data are courtesy of Servizio Idrologico –
482 Regione Toscana. E. Z and P. F acknowledge support from the Parthenope University
483 individual and group research funding.

484

485

486

487 **References**

488

489 Alvarez, A., Chiggiato, J., Mourre, B., 2012. Robotic characterization of access-restricted
490 marine environments. *IEEE Rob. Autom. Mag.*, 20 (3), 42-49.

491

492 Astraldi, M., Gasparini, G.P., Manzella, G.M.R., Hopkins, T.S., 1990. Temporal variability of
493 currents in the eastern Ligurian Sea, *J. Geophys. Res.*, 95(C2), 1515–1522.

494

495 Astraldi, M., Gasparini, G.P., 1992. The seasonal characteristics of the circulation in the
496 North Mediterranean basin and their relationship with the atmospheric climatic conditions. *J.*
497 *Geophys. Res.*, 97 (C6), 9531-9540.

498

499 Bosse, A., Testor, P., Mortier, L., Prieur, L., Taillandier, V., d’Ortenzio, F., Coppola, L.,
500 2015. Spreading of Levantine Intermediate Waters by submesoscale coherent vortices in the
501 northwestern Mediterranean Sea as observed with gliders, *J. Geophys. Res. Oceans*, 120,
502 1599–1622, doi:10.1002/2014JC010263.

503

504 Bouffard, J., Vignudelli, S., Cipollini, P., Menard, Y., 2008. Exploiting the potential of an
505 improved multimission altimetric data set over the coastal ocean, *Geophys. Res. Lett.*, 35,
506 L10601, doi: 10.1029/2008GL033488.

507

508 Ciuffardi, T., Napolitano, E., Iacono, R., Reseghetti, F., Raiteri, G., Bordone, A., 2016.
509 Analysis of surface circulation structures along a frequently repeated XBT transect crossing
510 the Ligurian and Tyrrhenian Seas. *Ocean Dynam.*, 66(6–7), 767–83.

511

512 Haidvogel, D.B., Arango, H., Budgell, W.P., Cornuelle, B.D., Curchitser, E., Di Lorenzo, E.,
513 Fennel, K., Geyer, W.R., Hermann, A.J., Lanerolle, L., Levin, J., McWilliams, J.C., Miller,
514 A.J., Moore, A.M., Powell, T.M., Shchepetkin, A.F., Sherwood, C.R., Signell, R.P., Warner,
515 J.C., Wilkin, J., 2008. Ocean forecasting in terrain-following coordinates: Formulation and
516 skill assessment of the Regional Ocean Modeling System. *J. Comput. Phys.*, 227: 3595-3624.
517
518 Manzella, G., 1985. Fluxes across the Corsica Channel and coastal circulation in the East
519 Ligurina Sea. *Morth-Western Mediterranean*, *Ocean. Acta*, 8 (1), 29-35.
520
521 Marchesiello, P., McWilliams, J. C., Shchepetkin, A. F., 2001. Open boundary conditions for
522 long-term integration of regional oceanic models. *Ocean Modell.*, 3, 1–20.
523
524 Menna, M., Gerin R., Bussani A., Poulain P.-M., 2017. The OGS Mediterranean Drifter
525 Dataset: 1986-2016. *Rel. OGS 2017/92 Sez. OCE 28 MAOS*, OGS, Trieste, Italy.
526
527 Moure, B., Chiggiato, J., 2014. A comparison of the performance of the 3-D super-ensemble
528 and an ensemble Kalman filter for short-range regional ocean prediction. *Tellus A*, 66, 21640.
529
530 Moure, B., Chiggiato, J., Lenartz, F., Rixen, M., 2012. Uncertainty forecast from 3-D super-
531 ensemble multi-model combination: Validation and calibration. *Ocean Dynam.*, 62(2): 283-
532 294.
533
534 Oddo, P., Adani, M., Pinardi, N., Fratianni, C., Tonani, M., and Pettenuzzo, D., 2009. A
535 nested Atlantic-Mediterranean Sea general circulation model for operational forecasting,
536 *Ocean Sci.*, 5, 461-473, doi:10.5194/os-5-461-2009.
537

538 Onken, R., Robinson, A.R., Kantha, L., Lozano, C.J., Haley, P.J., Carniel S. 2005. A rapid
539 response nowcast/forecast system using multiply-nested Ocean models and distributed data
540 systems, *J. Mar. Sys.*, 56, 45-66.
541

542 Pinardi, N., Masetti, E. 2000. Variability of the large-scale general circulation of the
543 Mediterranean Sea from observations and modelling: a review. *Palaeogeography,*
544 *Palaeoclimatology, Palaeoecology*, 158, 153-173.
545

546 Pinardi, N., Arneri E., Crise A., Ravaioli M., Zavatarelli M. 2006. The physical, sedimentary
547 and ecological structure and variability of shelf areas in the Mediterranean Sea. In: A. R.
548 Robinson and K. Brink (eds.), *The Sea*, Vol. 14 Harvard University Press, Cambridge, USA,
549 1245-1330.
550

551 Poulain, P.-M. 1999. Drifter observations of surface circulation in the Adriatic Sea between
552 December 1994 and March 1996, *J. Mar. Syst.*, 20, 231-253.
553

554 Poulain, P.-M. (2001), Adriatic Sea surface circulation as derived from drifter data between
555 1990 and 1999, *J. Marine Sys.*, 29, 3-32.
556

557 Poulain P.-M., Gerin R., Rixen M., Zanasca P., Teixeira J., Griffa A., Molcard A., De Marte,
558 M., Pinardi N. 2012. Aspects of the surface circulation in the Liguro-Provençal basin and
559 Gulf of Lion as observed by satellite-tracked drifters (2007-2009), *Boll. Geofis. Teor. Appli.*,
560 53(2), 261-279.
561

562 Poulain, P.-M. Gerin, R. 2019. Assessment of the water-following capabilities of CODE
563 drifters based on direct relative flow measurements. *J. Atmos. Ocean Tech.*, 36(4), 621-633,
564 doi: 10.1175/JTECH-D-18-0097.1

565

566 Vignudelli, S., Gasparini, G.P., Astraldi, M., Schiano, M.E. 1999. A possible influence of the
567 North Atlantic Oscillation on the circulation of the Western Mediterranean Sea, *Geophys.*
568 *Res. Lett.*, 26 (5), 623-626.

569

570 Vignudelli, S., Cipollini, P., Astraldi, M., Gasparini G.P., Manzella, G., 2000. Integrated use
571 of altimeter and in situ data for understanding the water exchanges between the Tyrrhenian
572 and Ligurian Seas. *J. Geophys. Res.*, 105 (C8), 19649-19663.

573

574 Shchepetkin, A.F., McWilliams, J.C., 2005. The regional ocean modelling system: a split-
575 explicit, free-surface, topography-following-coordinates ocean model. *Ocean Modell.* 9, 347–
576 404.

577

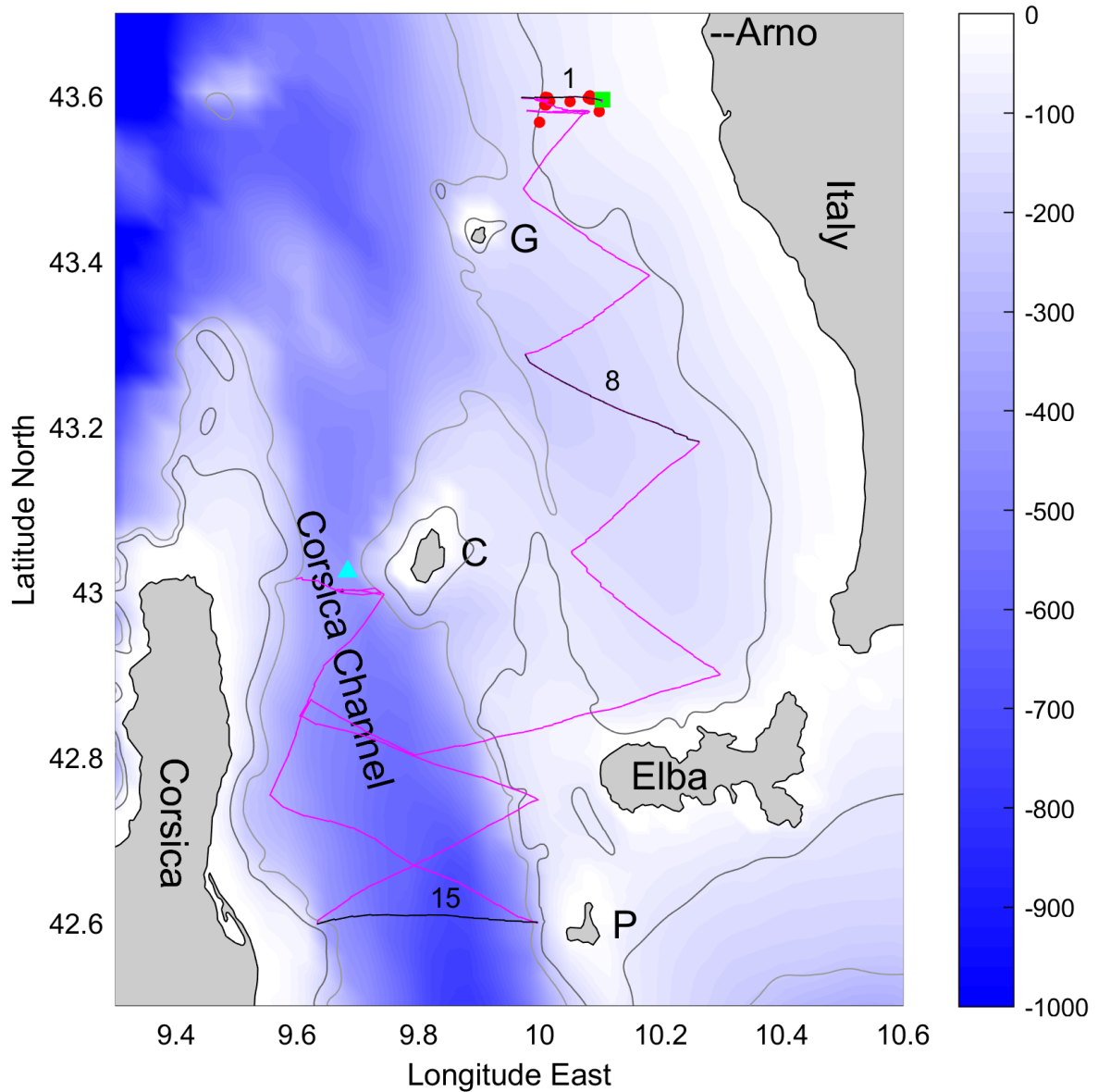
578 Vignudelli, S., Cipollini, P., Roblou, L., Lyard, F., Gasparini, G.P., Manzella G., Astraldi, M.
579 2005. Improved satellite altimetry in coastal systems: Case study of the Corsica Channel
580 (Mediterranean Sea), *Geophys. Res. Lett.*, 32, L07608, doi:10.1029/2005GL022602.

581

582 Schroeder, K., Chiggiato, J., Haza, A.C., Griffa, A., Özgökmen, T.M., Zanasca, P., Molcard,
583 A., Borghini, M., Poulain, P.-M., Gerin, R., Zambianchi, E., Falco, P., Trees, C. 2012.

584 Targeted Lagrangian sampling of submesoscale dispersion at a coastal frontal zone. *Geophys.*

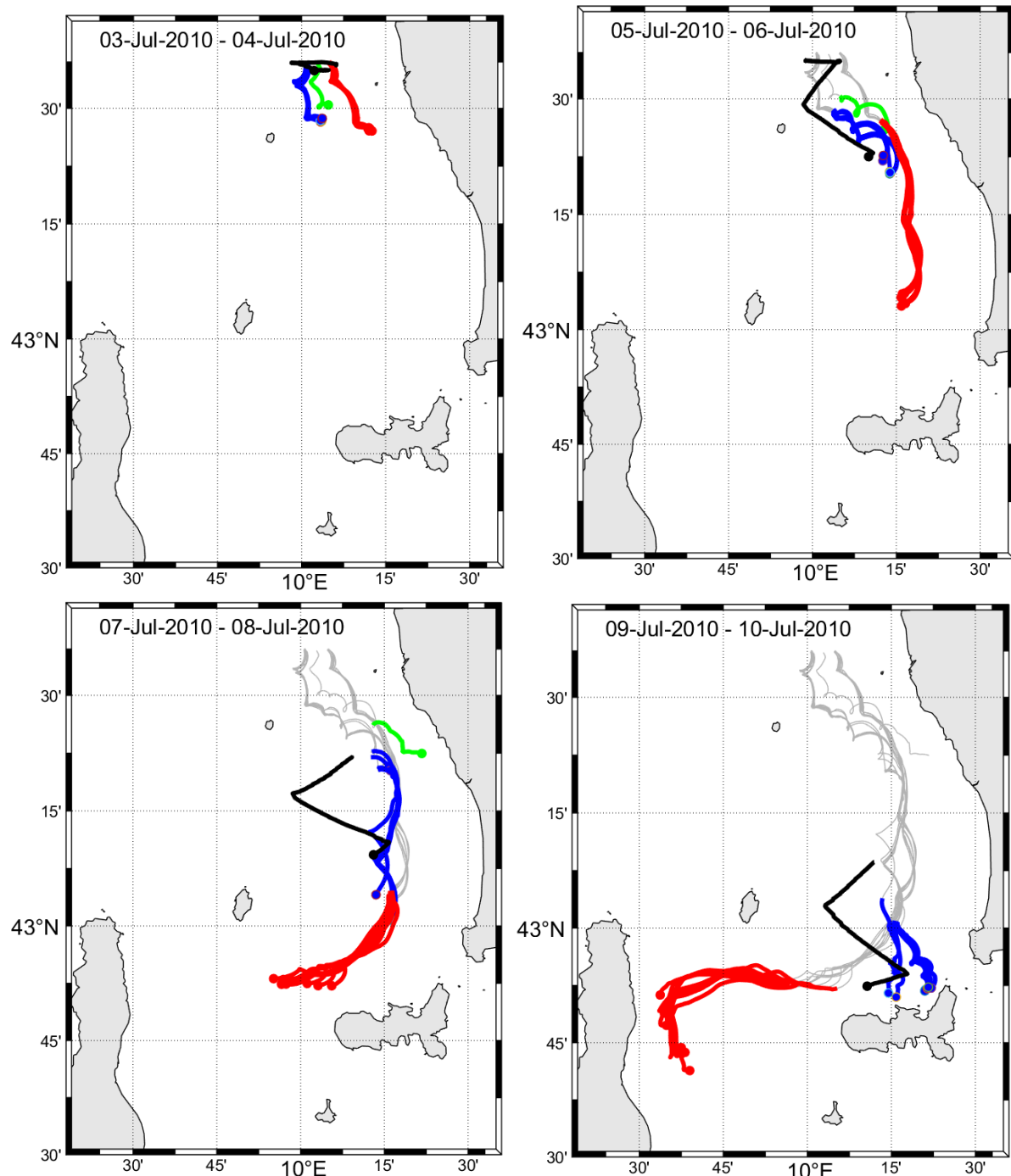
585 *Res. Lett.*, 39, L11608, doi:10.1029/2012GL051879.



586

587 Figure 1. Geography and bathymetry of the study area in the southeastern Ligurian and
 588 Corsica Channel. The Gorgona (G), Capraia (C) and Pianosa (P) islands are shown in addition
 589 to the Elba Island. The location of the CNR mooring is shown with a cyan triangle. The
 590 deployment locations of the drifters (red dots) and glider (green square) are also indicated.
 591 The glider track is shown in magenta, including the 3 transects (1, 8 and 15) described in the
 592 paper. Bathymetry is contoured (100 and 200 m) and shown with blue shades (m).

593



594

595

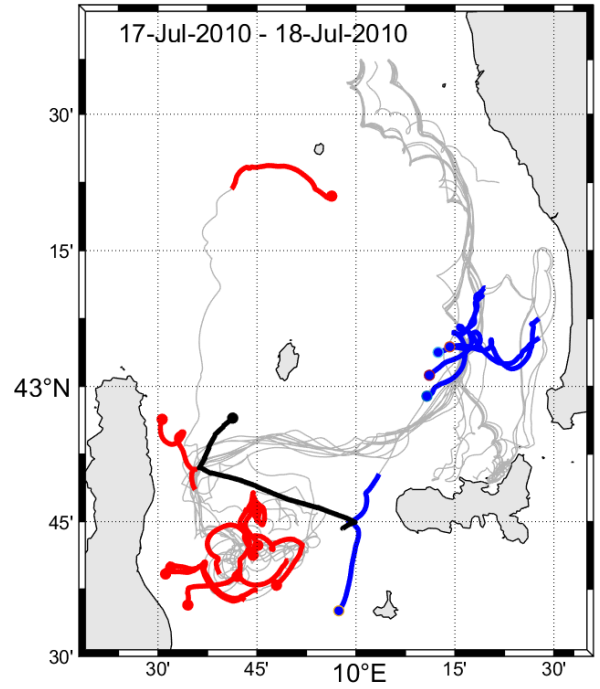
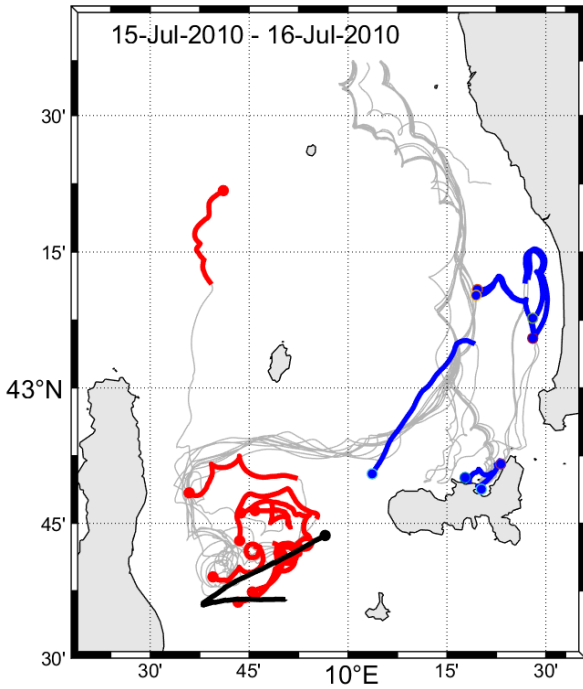
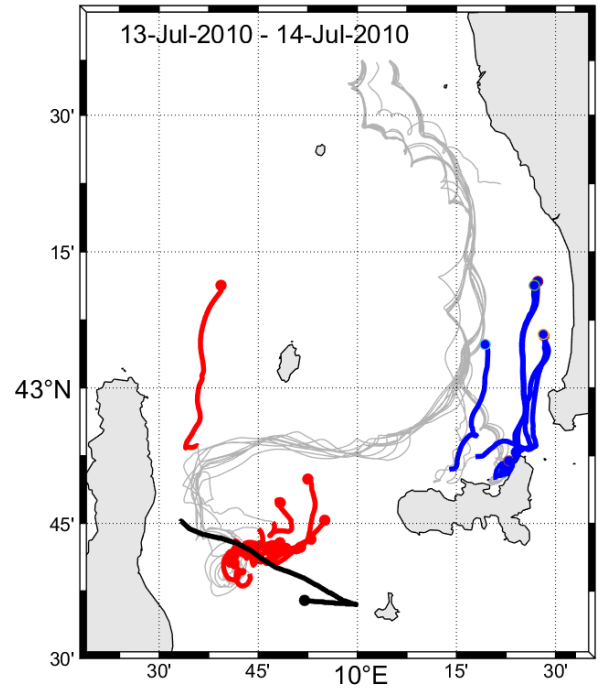
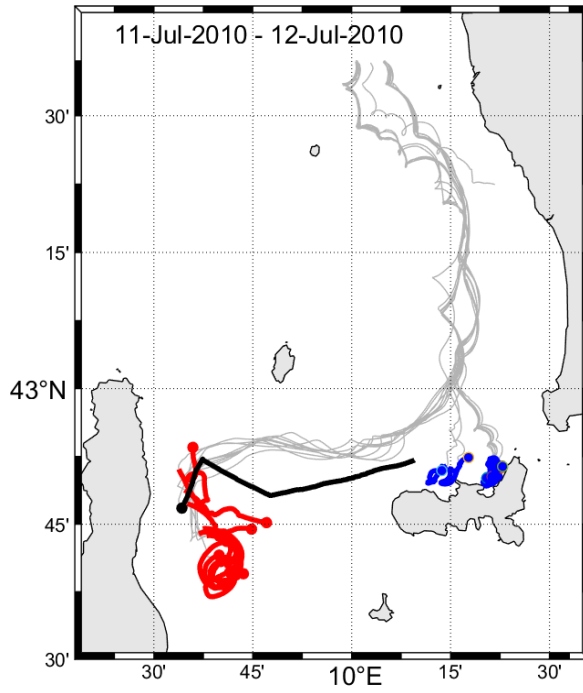
596

597

598

599

Figure 2. Two-day long drifter (red: coastal group; blue: outer group; green: intermediate drifter) and glider (black) track segments, with dot corresponding to the end of the second day, between 3 and 20 July. Cumulative tracks are shown in light grey shade.



600

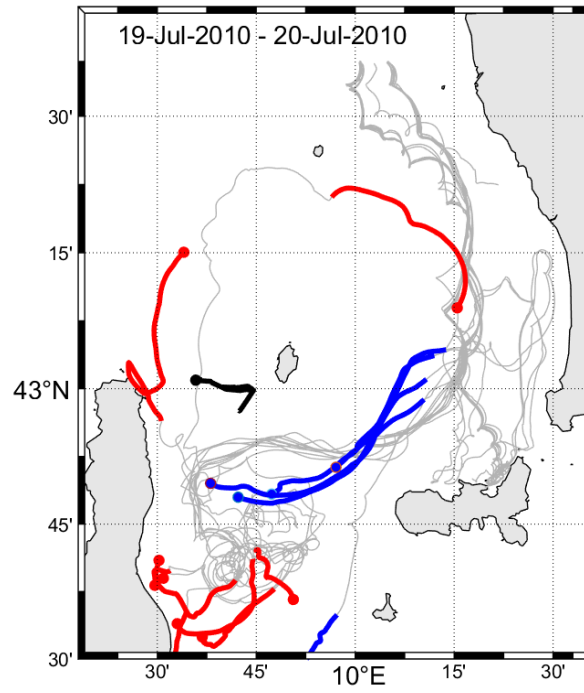
601

602

603

604

Figure 2. Continued.



605
606

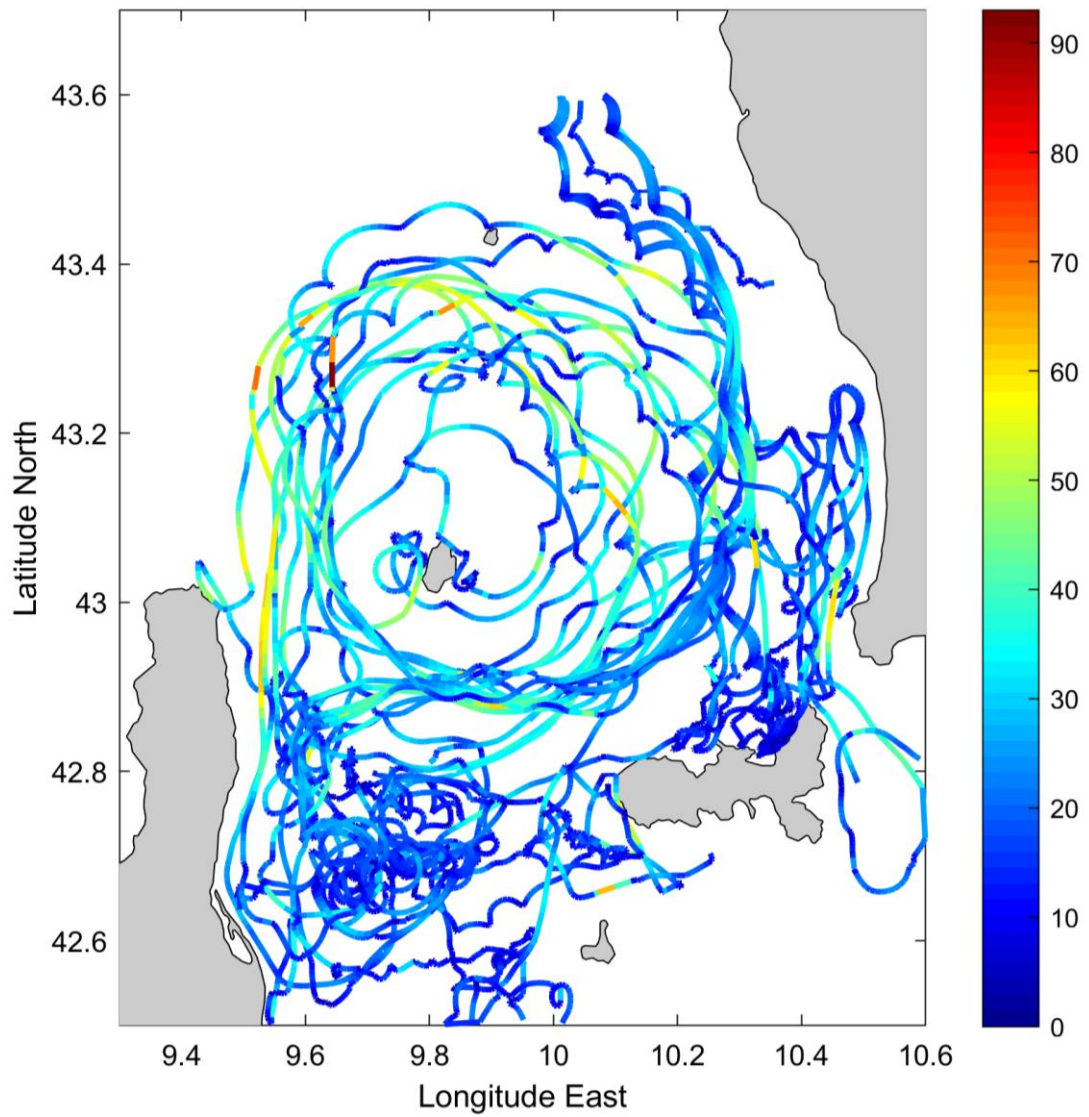
607

608

609

Figure 2. Continued.

610



611

612 Figure 3. Drifter trajectories for the period 3 July – 27 August 2010 color-coded as a function

613 of drifter speed (cm/s).

614

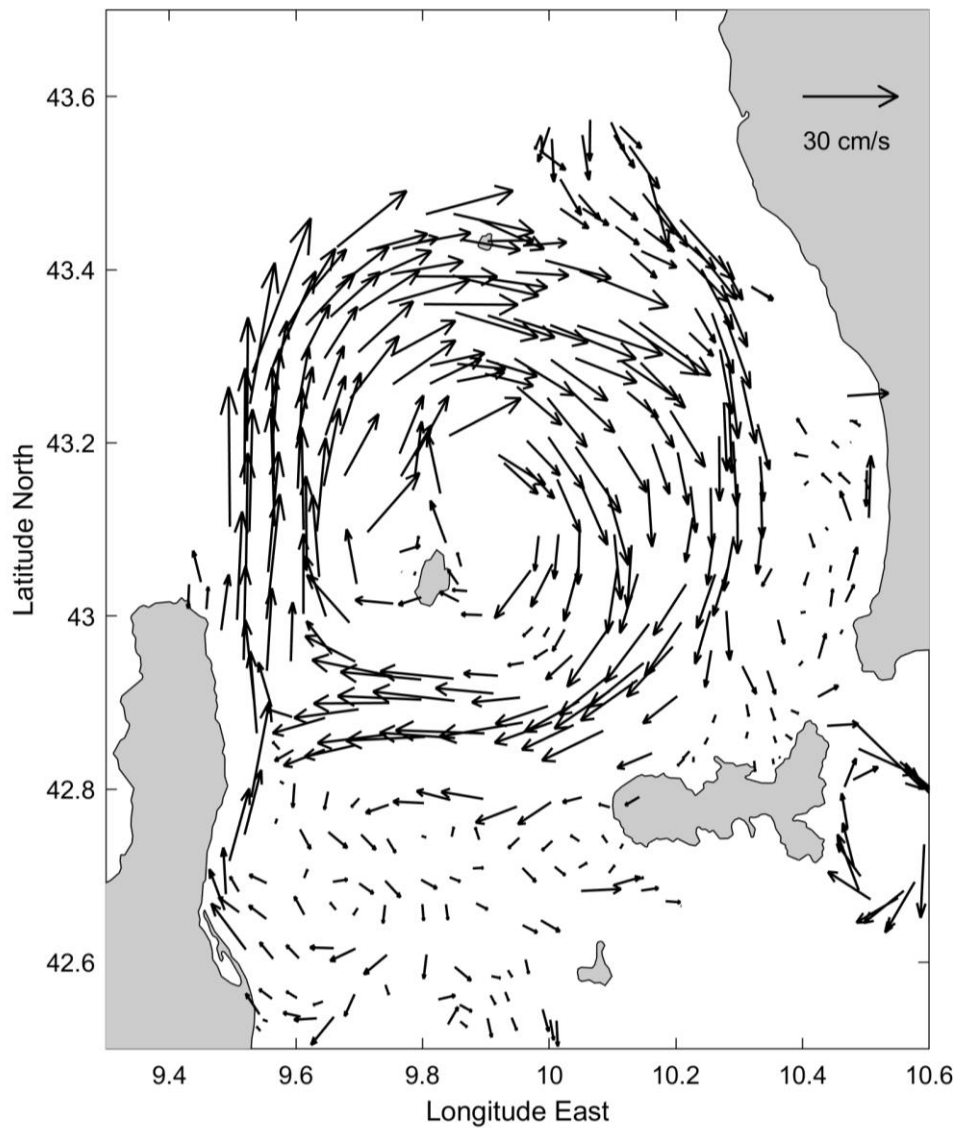
615

616

617

618

619



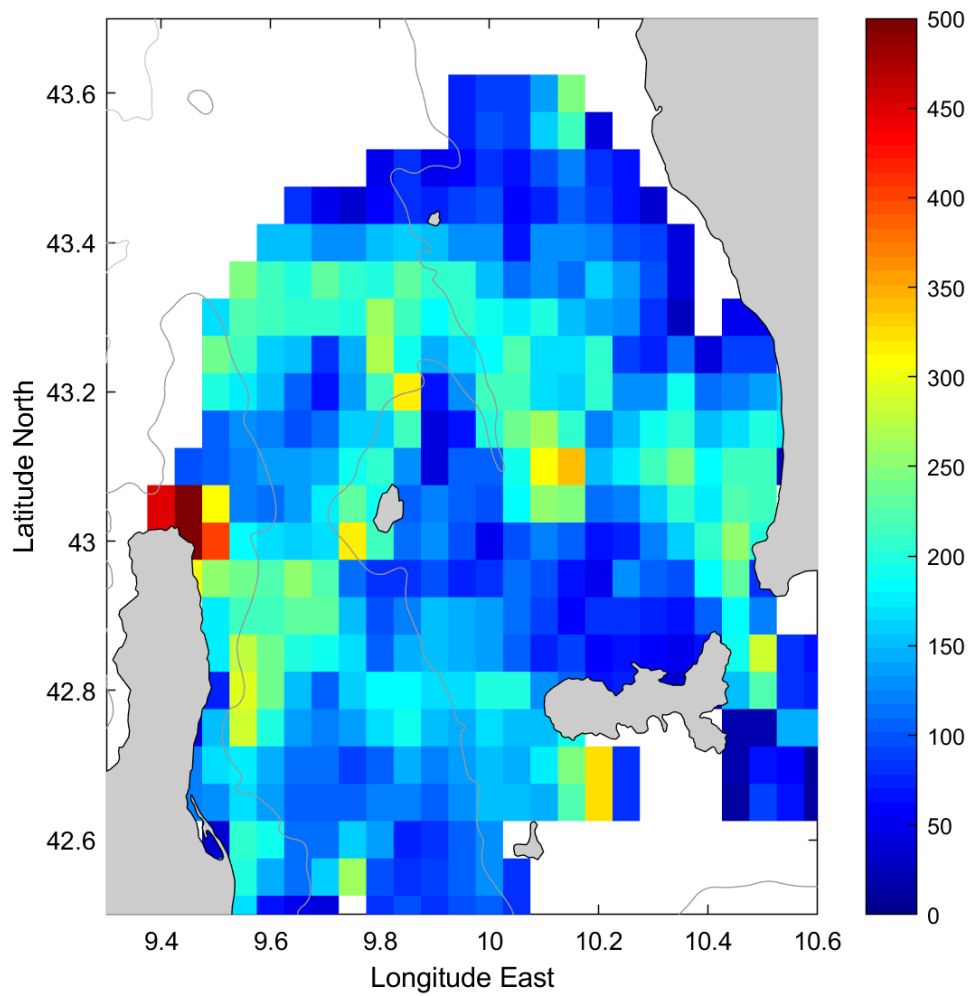
621

622

623 Figure 4. Mean surface circulation (arrows) and mean kinetic energy (colors, cm^2/s^2) in study
624 area for the period 3 July – 27 August 2010 using bins of $0.05^\circ \times 0.05^\circ$. Bins with less than 5
625 hourly observations were omitted.

626

627



629

630 Figure 5. Kinetic energy per unit mass of the velocity residuals or eddy kinetic energy (EKE,
631 $\text{cm}^2 \text{s}^{-2}$) in study area for the period 3 July – 27 August 2010 using bins of $0.05^\circ \times 0.05^\circ$. Bins

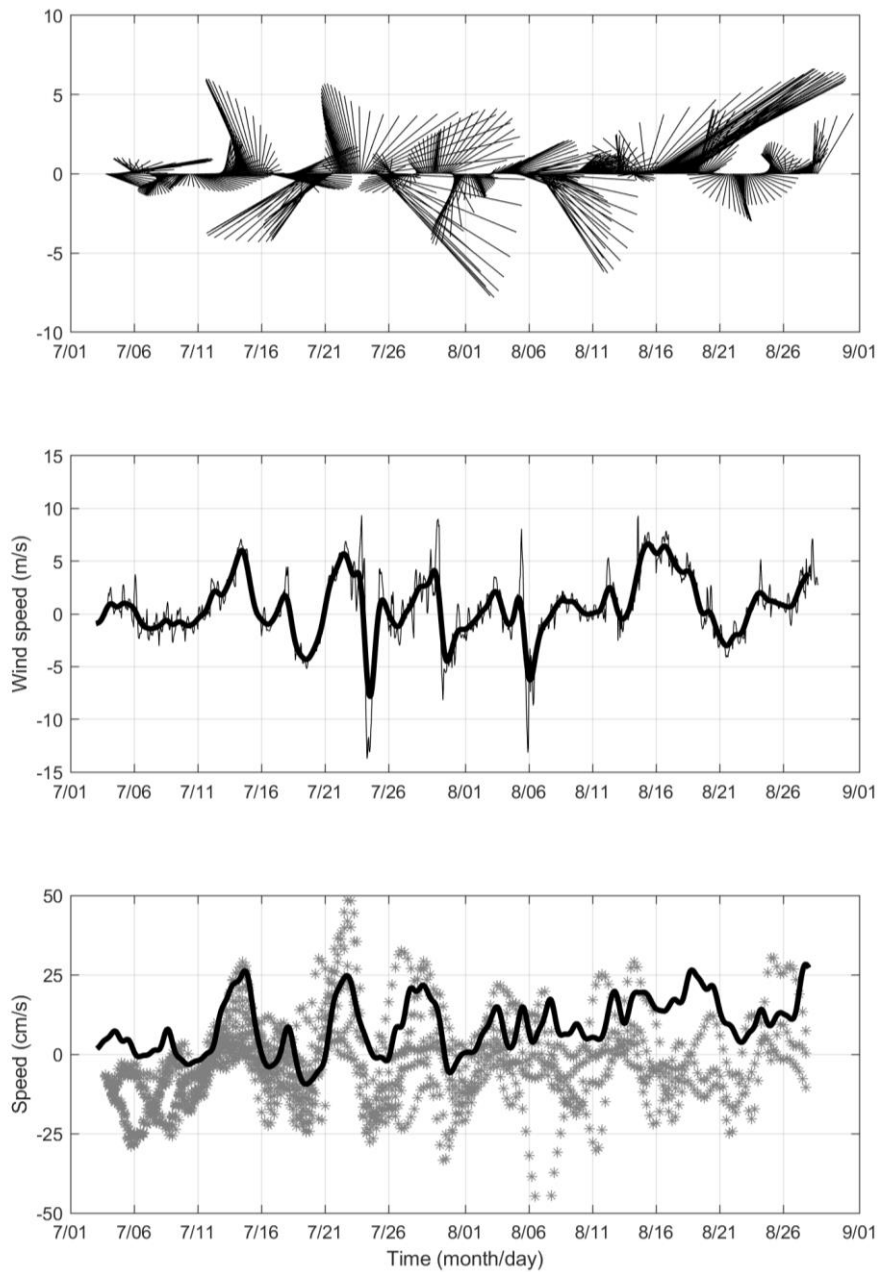
632

with less than 5 hourly observations were omitted.

633

634

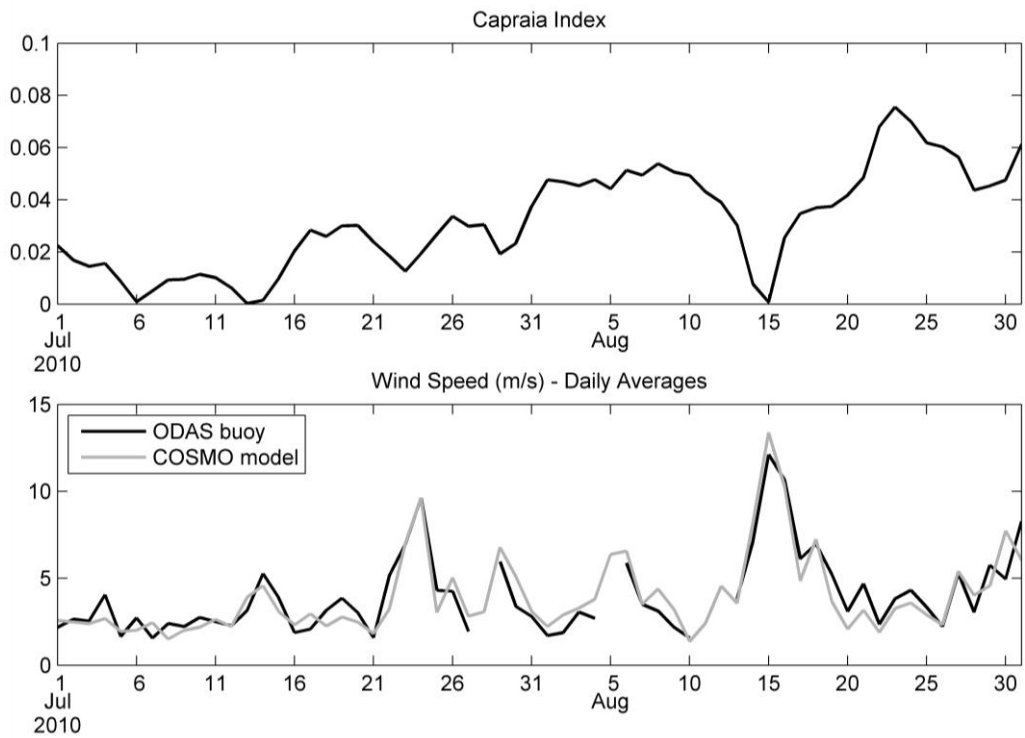
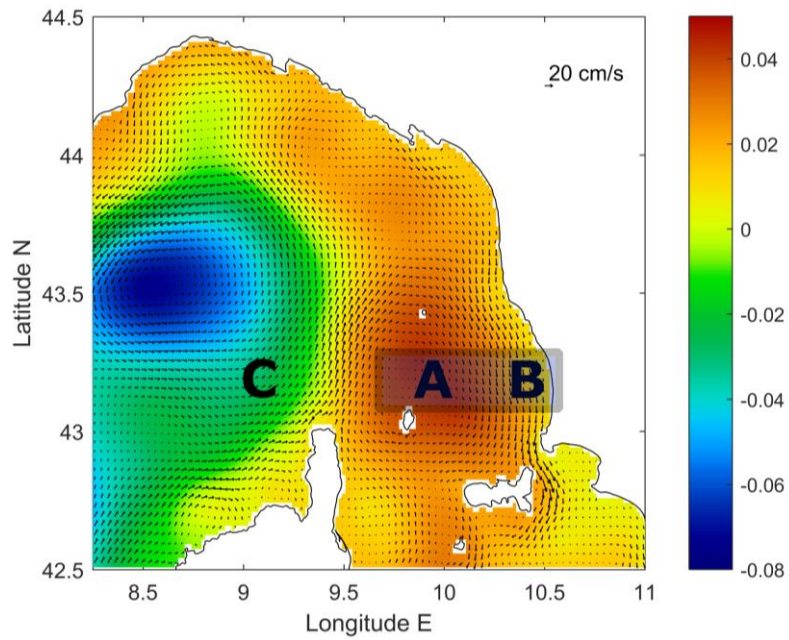
635



636

637 Figure 6. Stick diagram of the low-pass filtered COSMO-ME 10-m winds at grid point 43°
 638 7.5° N, $9^{\circ} 37.5^{\circ}$ E in the CC between 3 July and 27 August 2010 (top panel). Full (thin curve)
 639 and low-pass filtered (tick curve) COSMO-ME 10-m wind meridional component at the same
 640 location (middle panel). Low-pass filtered near-surface velocities at 32 m in the CC from
 641 mooring data (thick curve) and low-pass filtered velocities (light grey stars) of all the drifters
 642 in the study area (bottom panel).

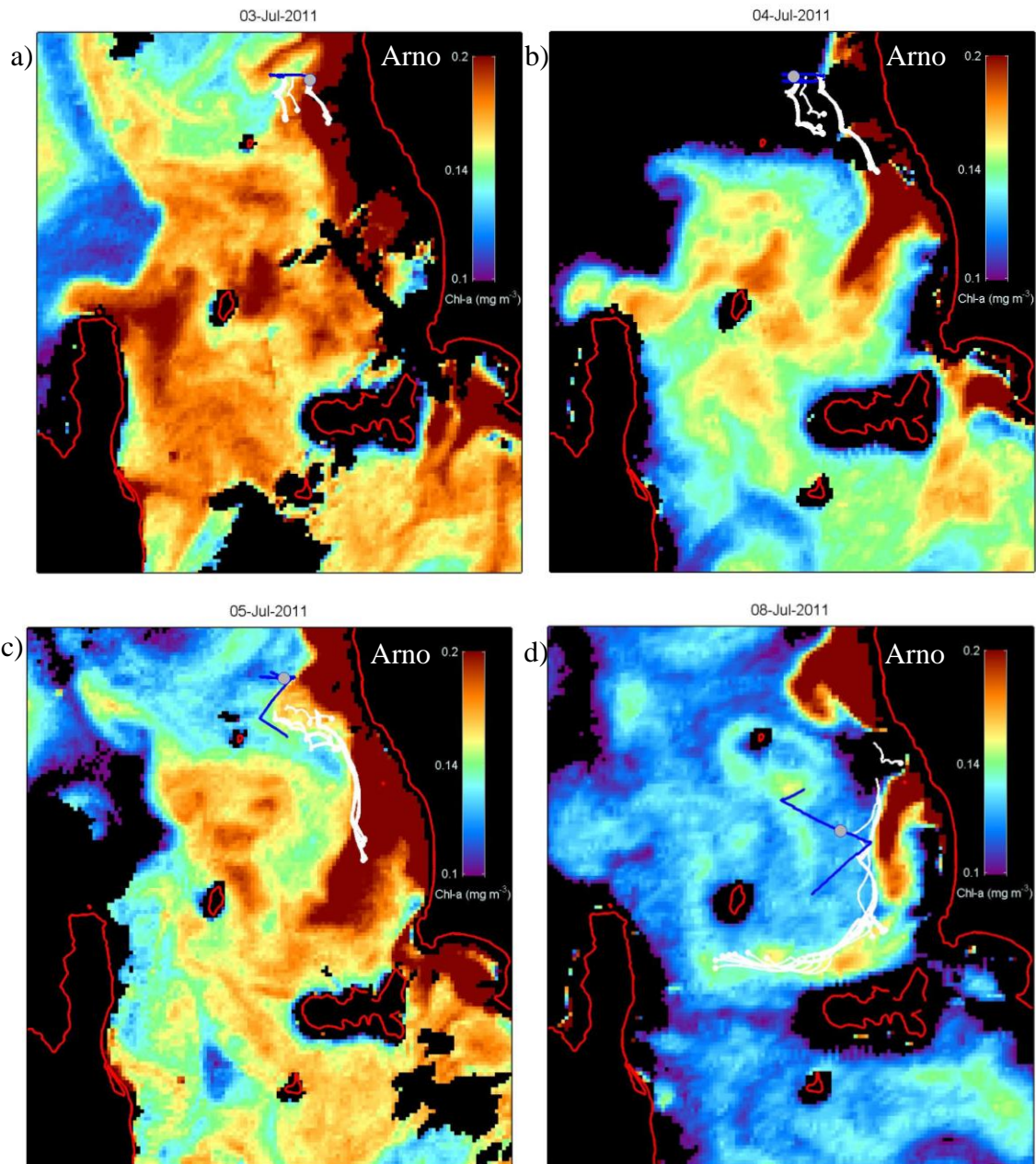
643



644

645 Figure 7. Ligurian Sea average circulation in July-August 2010 as simulated by ROMS (top
 646 panel). Colour is sea surface height (m) and arrows surface currents. Evolution of the daily
 647 average of the Capraia Index (m; middle panel) confronted to the daily average of COSMO-
 648 ME 10-m wind speed (m/s) at the ODAS buoy location and the measured ODAS 10-m wind
 649 speed (bottom panel).

650



651

652

653

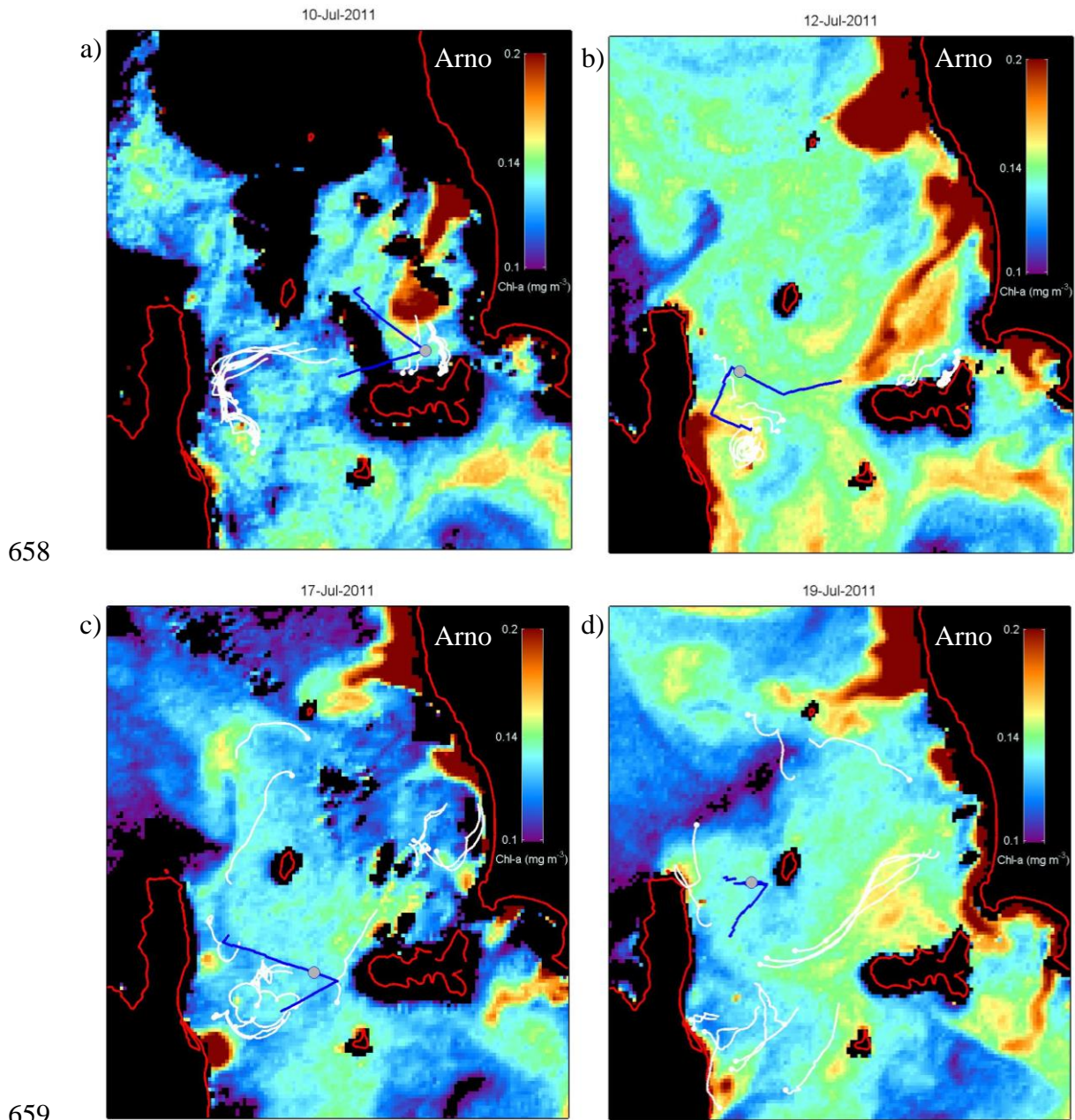
654

655

656

657

Figure 8. MODIS images of chlorophyll concentration on 3, 4, 5 and 8 July 2010, superimposed with centered 2-day long trajectories of drifters (white) and glider (blue). The gray dot represents the location of the glider at 12 GMT, contemporaneous with the satellite images.



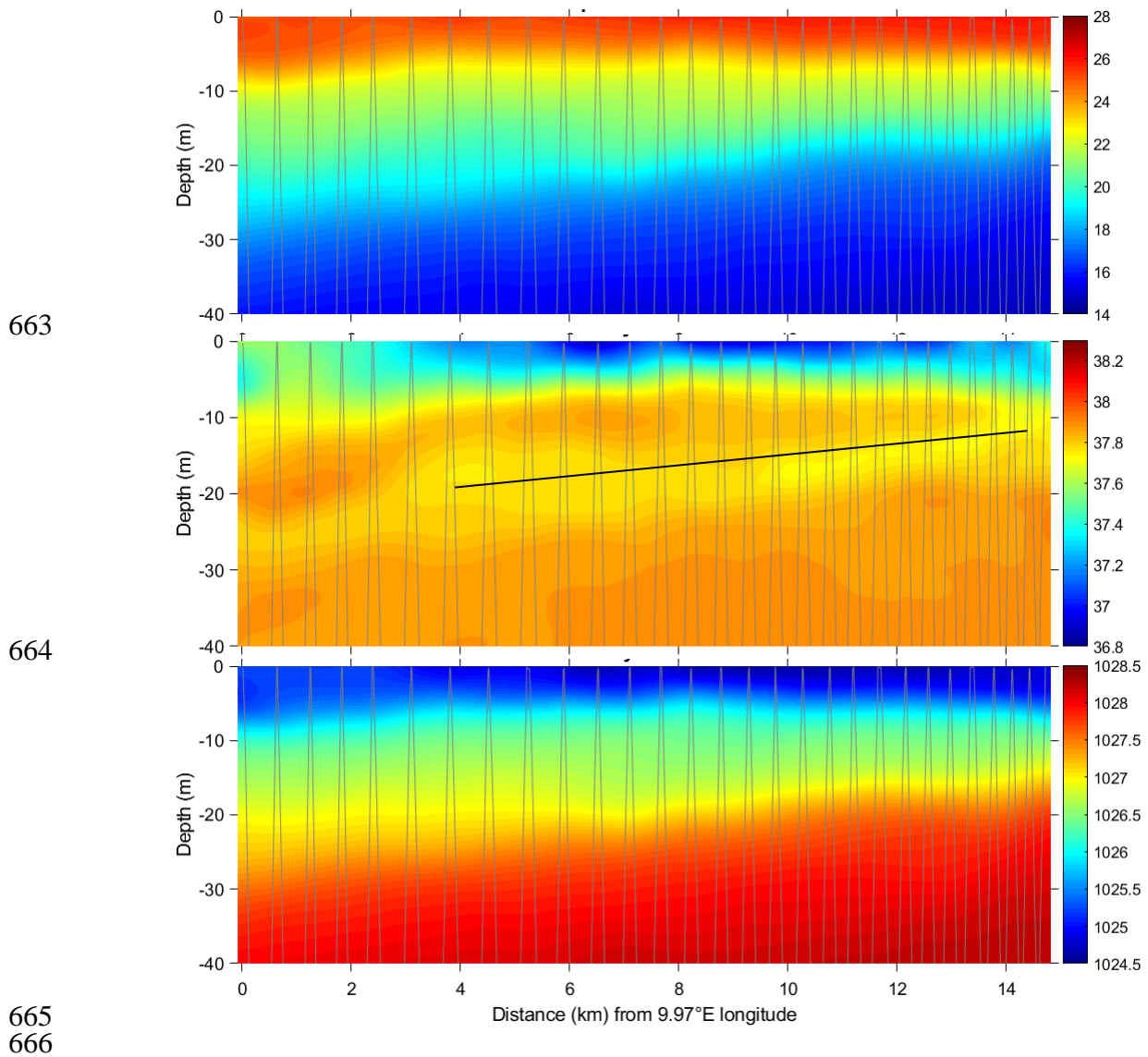
659

660

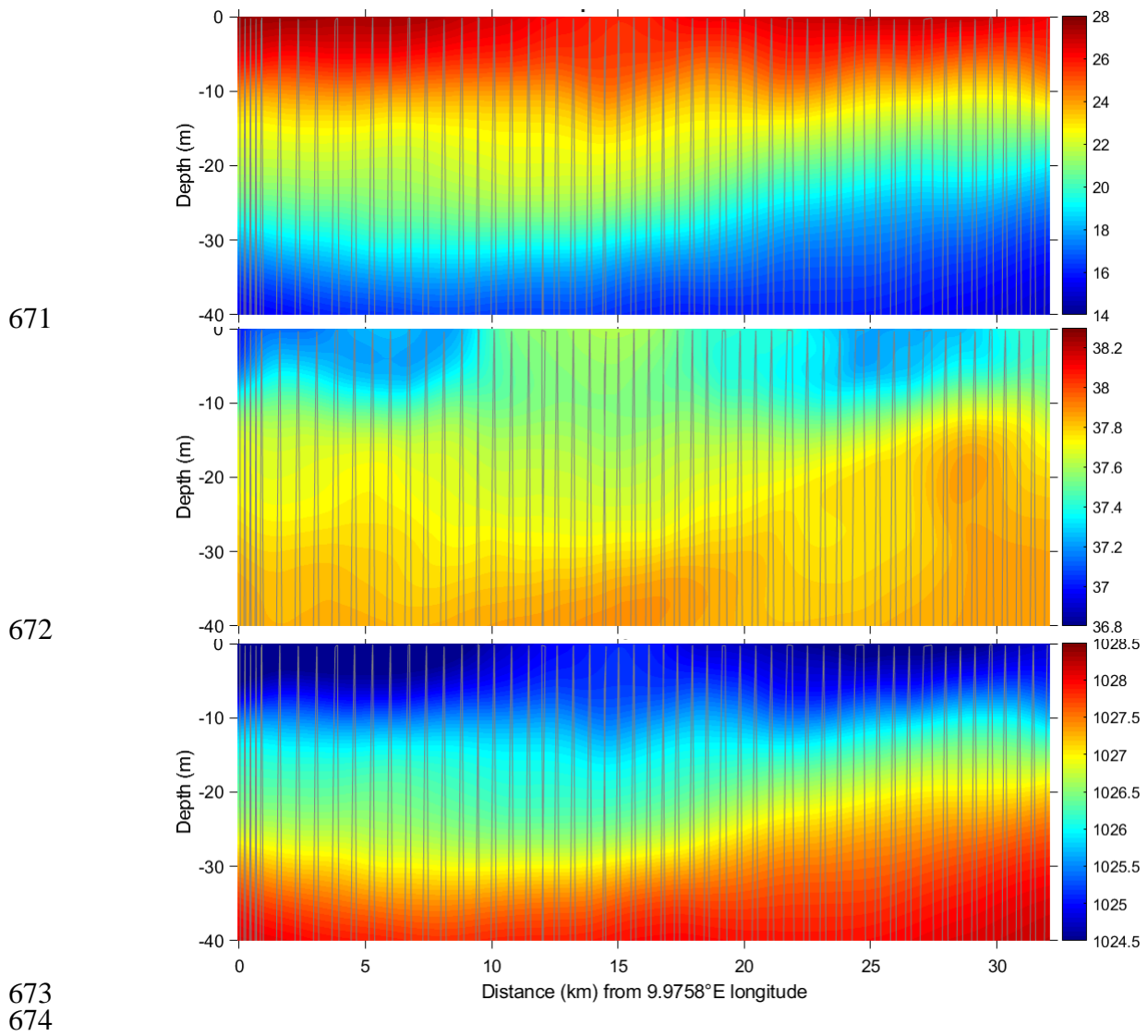
661

662

Figure 9. Same as Figure 8 but for 10, 12, 17 and 19 July 2010.



667 Figure 10. Contour plots of temperature ($^{\circ}\text{C}$, top), salinity (middle) and density (kg/m^3 ,
 668 bottom) versus depth and horizontal distance along glider transect 1. The origin is the
 669 westernmost location and the glider yo-yo track is shown with light grey lines. In the middle
 670 panel, a black line indicate subduction of less saline water along the isopycnals.



675 Figure 11. Same as in Figure 10 but for glider transect 8.

676

677

678

679

680

681

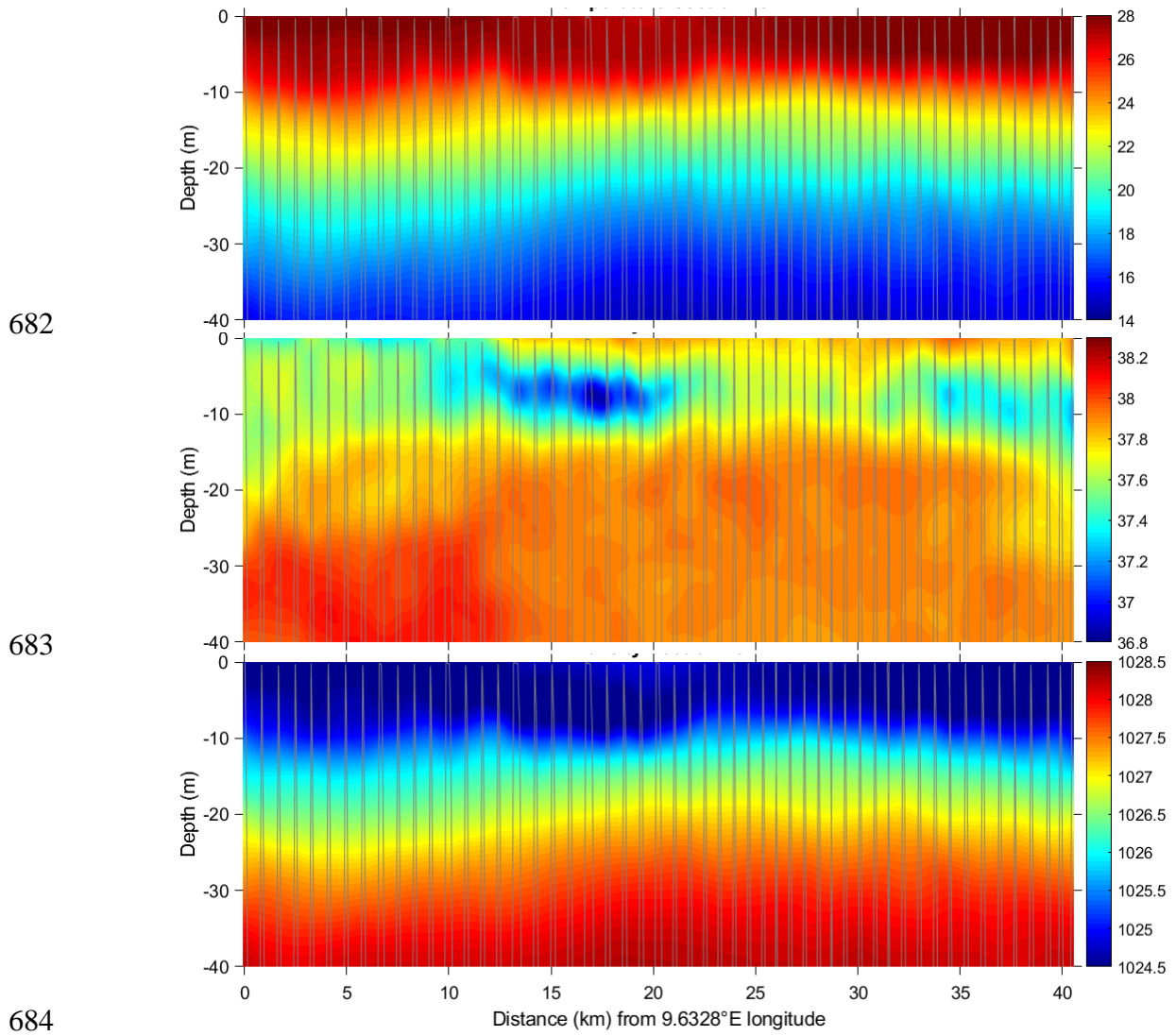
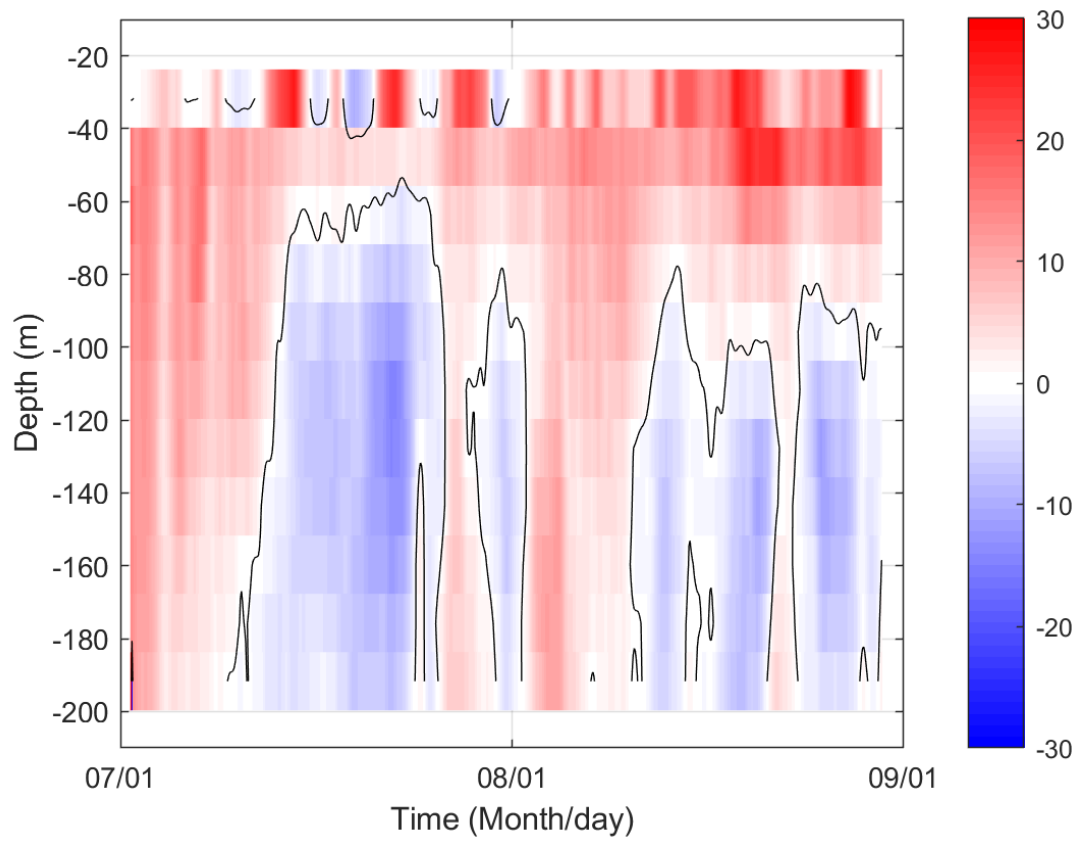


Figure 12. Same as in Figure 10 but for glider transect 15.



687

688

689 Figure 13. Meridional velocity (cm/s) measured by the moored ADCP in the CC (positive
 690 northward) as a function of time and depth above 200 m depth. The uppermost ADCP cell

691

was excluded. The null value is contoured with black curves.

692

693

694